# Classification of the Mobile Radio Propagation Environments Using Hidden Markov Models

Rafael Azevedo, Edson Cataldo

***Abstract*— The performance of wireless communication systems is primarily influenced by the mobile radio channel and its propagation mechanisms. This paper proposes an approach for characterizing wideband mobile radio channels based on hidden Markov model, in which the Viterbi algorithm is employed to provide a computationally efficient method for obtaining the likelihood sequence of hidden states (representing the radio propagation environments) from a set of observable states (channel temporal dispersion parameters). This approach enables the mobile radio channel classification into distinct transmission environments. The technique has proven to be a suitable option for statistically describing and classifying the wideband radio channel.**

***Keywords*— *Hidden Markov model, mobile radio channel, swept-frequency technique, time dispersion parameters, Viterbi algorithm.***

## I. INTRODUCTION

Wireless communication systems have evolved over generations to support a wide range of devices and services, addressing the current demands of various market segments [1]. In fact, the mobile radio channel (MRC) and its propagation mechanisms impose significant limitations on the performance of radio communication systems [2] [3]. Therefore, comprehensive knowledge and understanding of different types of MRC have become critical skills for the design and optimization of modern high-performance wireless communication systems.

In this context, this paper proposes the application of the hidden Markov model (HMM) technique and the Viterbi algorithm to classify distinct transmission environments, based on the characterization of the wideband MRC within each propagation scenario. This research builds upon previous studies [4] [5] [6], in which HMMs were employed to statistically characterize wideband MRCs in different locations, using the main temporal dispersion parameters of the MRC (average delay and delay spread) and yielding positive results.

The organization of this paper is as follows: Section II exposes succinctly the characterization of the MRC, the HMM application, and the Viterbi algorithm. Section III briefly details the measurement setup, the environment of the measurement campaign, and data collection process. Section IV describes the proposed methodology to apply the HMM and Viterbi algorithm in MRC classification. Section V starts by presenting the evaluations, and then evaluates the results. Section VI summarizes the ideas discussed throughout the paper, presents the conclusions, and outlines some suggestions for further research.

Rafael Azevedo, e-mail: rafaelazevedo@id.uff.br; Edson Cataldo, e-mail: ecataldo@id.uff.br; Telecommunications Engineering Department, Fluminense Federal University, Niterói-Rio de Janeiro, Brazil.

## II. CHARACTERIZATION OF THE MOBILE RADIO CHANNEL AND HIDDEN MARKOV MODEL

### A. Characterization of the mobile radio channel

Radio waves propagate through the mobile radio channel (MRC) and are mainly influenced by physical and natural phenomena known as propagation mechanisms, which describe the effects of reflection, scattering, and diffraction [2]. These propagation mechanisms generate multiple waves that travel along the radio link path until reaching the destination. The superposition of these waves, each one propagating along different paths with distinct amplitudes, phases, and delays, constitutes the received signal.

In this context, radio waves may propagate through a direct line-of-sight (LOS) path between transmitter and receiver, or, more commonly, experience non-line-of-sight (NLOS) propagation, encountering various obstacles such as buildings, trees, vehicles, pedestrians, and mountains. These obstacles give rise to multiple propagation paths, characterizing what is referred to as a multipath environment [2].

The received signals resulting from the superposition of multiple radio waves at the receiving antenna exhibit attenuation and fluctuations in amplitude, a phenomenon known as fading. Fading can be categorized into large-scale fading (associated with path loss and shadowing) and small-scale fading (related to localized variations over distances on the order of half a wavelength) [3].

Due to the effects of large-scale and small-scale fading, the radio link experiences constructive and destructive interference, leading to the formation of distinct propagation environments and, consequently, affecting the characteristics of the MRC. Therefore, the MRC and its associated propagation mechanisms have a significant impact on wireless communication systems, often limiting their performance.

As a result, the design and evolution of mobile communication systems must carefully consider the adverse impacts of the MRC. Proper channel characterization and dimensioning are essential for achieving more effective, reliable, and high-performance wireless systems.

### B. Hidden Markov model technique

Although there is an extensive range of applications for Markov chains, the focus of this paper is on phenomena that are not directly exposed to observers. In such cases, states of the Markov chain are called hidden states, and thereby inferences about a particular phenomenon are only unveiled by examination of secondary incidents designated as observable states [7]. Thus, the hidden Markov Model (HMM) technique involves the adoption of two distinct stochastic processes: the layer of hidden states constitutes the unobservable Markov chain (satisfying the Markov property), and the layer of

observable states represents the visible outputs, which are linked with each hidden state or associated with each transition between hidden states, and therefore are entirely dependent on the random activities of the hidden states [8]. Transitions between hidden states follow a probabilistic set of rules and usually assume the most common form of a first-order Markov chain, exposing the observable states while flowing between hidden states. So, the evolution of random incidents that represent the observable states (visible outputs) indicates indirectly the evolution of the hidden states.

Different research efforts have adopted the HMM technique [4] [9] [10]. It appears as a strong mathematical tool basis to model time series, characterizing complex systems with temporal elements, which can be subjected to noises or other sources [11]. Given a time interval T, in which there are discrete and finite numbers of the generic time instant t, HMM can be represented as follows:

$T$-long sequence of hidden states $s$ is indicated as the set of hidden states $S = (s_1, s_2, \dots, s_T)$.

$T$-long sequence of observed states $y$ is pointed out as the set of observable states $Y = (y_1, y_2, \dots, y_T)$.

Transition probability from the hidden state $s_i$ to $s_j$ is represented by $a_{ij}$. The set of hidden state transitions leads to $S$ by $S$ row-stochastic matrix named state transition probability matrix $A$, which is a square matrix with dimensions $S$ by $S$, and the sum of its rows is always equal to one, $\sum_{j=1}^{N} a_{ij} = 1$. Matrix $A$ is depicted below.

$$A = \begin{bmatrix} a_{11} & a_{12} & \cdots & a_{1N} \\ a_{21} & a_{22} & \cdots & a_{2N} \\ \vdots & \vdots & \ddots & \vdots \\ a_{N1} & a_{N2} & \dots & a_{NN} \end{bmatrix} \quad (1)$$

Transition probability to hidden state $s_j$ leads to probability distribution of the observable state that is represented by $b_j$, mapping the sequence of hidden states into observable states sequence. The group of observed states $b_j$ results to a rectangular matrix $B$ named emissions matrix or observation probability matrix. As is true for matrix $A$, the sum along the matrix $B$ rows is equal to one, $\sum_{j=1}^{M} b_j = 1$. Matrix $B$ is depicted below.

$$B = \begin{bmatrix} b_{11} & b_{12} & \cdots & b_{1M} \\ b_{21} & b_{22} & \cdots & b_{2M} \\ \vdots & \vdots & \ddots & \vdots \\ b_{N1} & b_{N2} & \dots & b_{NM} \end{bmatrix} \quad (2)$$

Initial hidden state referred to as $r_i$, in which the elements describe the probability distribution of the initial model in the time instant represented as $t = 1$. The collection of these elements leds to initial state distribution $R = \{r_i\}$ for $i = 1, \dots, N$ in which $r_i = P(q_t = s_i)$ in $t = 1$. $R$ is defined as a start probability vector which is filled out with initial probability of the discrete hidden states.

$$R = [r_1 \quad r_2 \quad \dots \quad r_N] \quad (3)$$

In the light of the above, a complete specification of HMM can be summarized as:

$$\mathrm{M_{HMM}} = (\mathrm{A}, \mathrm{B}, \mathrm{R}) \quad (4)$$

In the context of the HMM, it is possible to consider three significant problems [11]: evaluation (computing the probability of an observation sequence), estimation (finding the most likely hidden state sequence), and training (learning the model parameters). The fundamental challenges listed above are the core computational tasks when dealing with HMM, as shown in Table I. It is possible to address all three computational challenges, depending on the specific application, or the main focus can vary based on what it is trying to achieve. This paper focus attention on the estimation problem (decoding problem) trying to uncover the likeliest sequence of hidden states from a set of observable states.

TABLE I. *THREE BASIC PROBLEMS FOR HMM [11].*

| Problem name | Description |
|---|---|
| 1. Evaluation problem | Given the sequence of observed states $Y$ and the model $M_{HMM}$, how to compute the $P(Y \vee M_{HMM})$?<br>Solution: forward-backward algorithm. |
| 2. Estimation or decoding problem | Given the sequence of observed states $Y$, how to compute the optimal (in some meaningful sense) sequence of hidden states $S$?<br>Solution: Viterbi algorithm. |
| 3. Training problem | How to change slightly the model parameters $M_{HMM} = (A, B, R)$ to achieve the maximization of $P(Y \vee M_{HMM})$?<br>Solution: Baum-Welch algorithm. |

### C. The Viterbi Algorithm

The Viterbi algorithm can be associated with the operation of discrete HMM and provides computational and efficient method to achieve the a posteriori likeliest sequence of hidden states, given a set of observed incidents. In other words, this algorithm takes advantage of the recursion process to compute the most likely sequence of hidden states that generated a given observation sequence. Instead of keeping track of all paths during execution, the Viterbi algorithm computes the ideal subpaths and discards the others subpaths while it crosses the sequence of observed states.

The algorithm starts with definition of $\delta_t(i)$ and $\psi_1(j)$. Out of all possible sequences of hidden states leading up to $S_i$ at time $t$, $\delta_t(i)$ calculates the highest probability of ending up at this state $S_i$ at time $t$. In addition the array $\psi_1(j)$ is used to keep track of the computed maximum values in $\delta_t(i)$. This Viterbi algorithm can be described in the following steps:

Initialization:

$$\delta_1(i) = r_i b_i(y_1) \quad 1 \le i \le N$$
$$\psi_1(i) = 0 \quad (5)$$

Recursion:

$$\delta_t(j) = max_{1 \le i \le N}\left[\delta_{t-1}(i) a_{ij}\right] b_j(y_t)$$
$$2 \le t \le T \; and \; 1 \le j \le N \quad (6)$$

$$\psi_t(j) = argmax_{1 \le i \le N}\left[\delta_{t-1}(i) a_{ij}\right]$$
$$2 \le t \le T \; and \; 1 \le j \le N \quad (7)$$

Termination:

$$P = max_{1 \le i \le N}[\delta_T(i)] \quad (8)$$

$$q_T = argmax_{1 \le i \le N}[\delta_T(i)] \quad (9)$$

Backtracking path:

$$q_t = \psi_{t+1}(q_{t+1})$$
$$t = T-1, T-2, \dots, 1 \quad (10)$$

## III. MEASUREMENT CAMPAIGN

### A. Measurement setup

The swept-measurement technique has been adopted. It is a channel sounding method in the frequency domain, limited to shorter distances because the receiving and transmitting antennas have to be connected to the same vector network analyzer (VNA) equipment [2]. A total of 1,601 sinusoidal signal samples of 10 dBm amplitude was generated and transmitted, successively, in discrete frequencies and equally spaced along a frequency band of 750 MHz (from 960 MHz to 1,710 MHz). Through the input port, the transceiver VNA completely swept the frequency band with the respective 10 dBm sinusoidal carriers and, in parallel, monitored the output port, providing the transfer function of the channel (channel impulse response) in the frequency domain. 60-meter coaxial cable was used, permitting to perform measures in short distances, of up that value. The main parameters of the measurement setup are indicated in Table II.

TABLE II. *CHANNEL SOUNDING PARAMETERS [12].*

| Parameters | Value | Unit |
|---|---|---|
| Frequency band | 960 to 1,710 | MHz |
| Bandwidth | 750 | MHz |
| Transmitted power level | +10 | dBm |
| Low Noise Amplifier (LNA) gain | 25 | dB |
| Antennas gain | 2,14 | dBi |
| Frequency resolution ($\Delta f$) | 0.46875 | MHz |
| Sweep-measuring samples | 1,601 | - |
| Sweep-measuring time | 696 | ms |
| Delay resolution ($\Delta\tau$) | 1,333 | ns |
| Maximum delay ($\tau_{MAX}$) | 2,133 | ns |

The proper equipment was as follow [12]: broadband omnidirectional antennas with discone design that were positioned 1.5 m above the ground; VNA (model Hewlett Packard HP8714ET); HP acquisition board to connect the VNA to laptop with Matlab software interface; laptop to control the measurement campaign and save all measure data; low noise amplifier (LNA, model MINI-Circuits ZLR-2150); voltage supply 12VCC to energy the LNA; HPIB cable (Hewlett Packard Interface Bus); N-type and SMA-type connectors and coaxial cables (models RG-213 and RG-58U).

The system was properly calibrated before each measurement campaign to secure the compensation for equipment losses and, moreover, the transmitter and receiver were synchronized. Therefore, all data recorded during the measurement campaign corresponded entirely to the behavior of the propagation channel.

### B. Environment of the measurement campaign and data collection process

The measurement campaign was conducted on the Praia Vermelha Campus from Fluminense Federal University, located in Niterói city, state of Rio de Janeiro, Brazil. The campaign was performed on the third floor inside the building and outside, in an opened corridor, connecting the building block D to another building block E. The opened environment between the buildings is surrounded by stone benches, a garden on a sloping area and trees.

As illustrated in Figure 1, the transmitter (TX) and receiver (RX) were set up in different positions to capture the channel transfer function at different scenarios. The environment was previously selected for the measurement campaign and correspond to so-called indoor, transition environment from internal to external place (indoor-outdoor), and vice versa (outdoor-indoor).

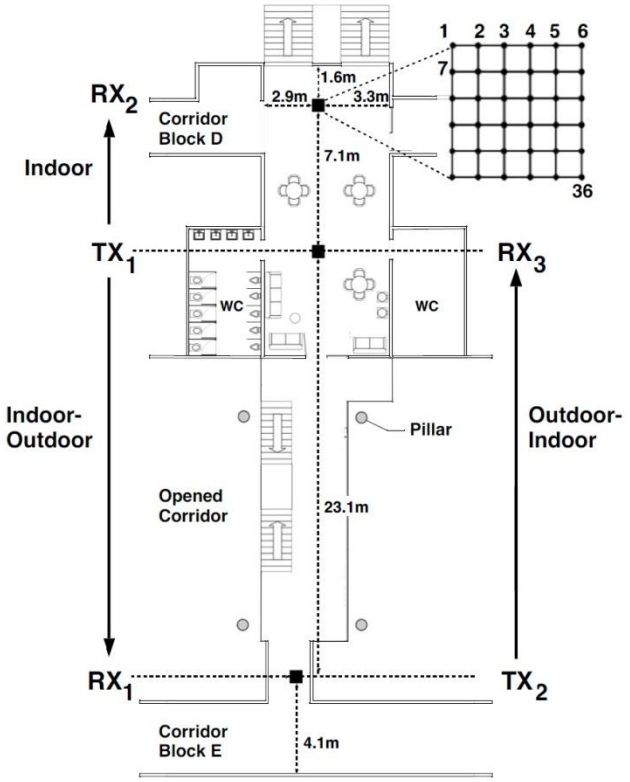


Fig. 1. Plant layout - Third floor building, UFF Praia Vermelha Campus.

At this selected environment, the reception was set up to capture the channel transfer function at different positions, which shall be appointed as RX. For each location RX, a 6-by-6 quadrangular grid was set up, mapping 36 reception dots equally spaced by 15 cm [12]. For wideband frequency (750 MHz bandwidth), in which the values of $\lambda$ ranged between 17.54 cm (upper frequency of 1,710 MHz) and 31.25 cm (lower frequency of 960 MHz), given that 0.38 $\lambda$ is the necessary distance between uncorrelated samples [3], the spacing of 15 cm was calculated to ensure that the measurements of the 36 dots of each location RX were not correlated. Hence, the equally spaced dots, set apart by 15 cm in the grid, were sufficient to guarantee the de-correlation at signal reception among the 36 dots.

The measurements of the channel transfer function at each dot were performed in a row, one after the other until reaching the 6-by-6 quadrangular grid at each location RX. In each dot, during the frequency sweep of 696 ms, a set of 1,601 samples of 10 dBm equally spaced swept completely the 750 MHz bandwidth, thereby generating 1,601 impulse responses that were recorded and saved on local laptop. This stored database was preprocessed and treated to achieve, in the time domain, a set of 1,601 samples of the channel impulse response. Based on this information, the temporal dispersion parameter of the MRC (average delay $\tau_m$) were reached.

It is important to emphasize that during the frequency sweep of 696 ms, which was entirely treated as a time instant, special attention and all necessary precautions were put in

place to ensure the MRC remained static. Measurements were carried out during least busy hours (weekends and evening late or early morning) and researchers ensured no movement of people and themselves surrounding the measurement site on the time instant of frequency sweep [12]. Therefore, no changes in the environment were seen during the frequency sweep of 696 ms, guaranteeing an instantaneous measurement.

## IV. RESEARCH METHODOLOGY

### A. Data acquisition and preprocessing from MRC

Due to the dual relationship between time and frequency domains, it was possible to measure the channel impulse response in the frequency domain (via swept-measurement technique) [2] and the main temporal dispersion parameters of the MRC in the time domain were provided indirectly.

Each reception location appointed as RX captured the channel frequency responses and, for each RX, it was used a 6-by-6 quadrangular grid. By taking into account the 36 measurements of impulse response performed in a row as the concatenation of short events, in which it was regarded that the variables assumed discrete values and the autocorrelations were invariant during short temporal transitions [3], it was admitted to design each RX as a radio channel named Quasi-Wide-Sense Stationary Uncorrelated Scattering (QWSSUS).

For each moment, each dot in the 6-by-6 quadrangular grid, the data corresponded to the responses of the channel through the frequency sweep with sinusoidal carriers and, therefore, related to the channel transfer function $T(f,t)$ defined as the MRC frequency response for each moment, each point in time [3]. Since the channel was considered a linear filter, the input and output records were characterized directly by $T(f,t)$. The 3-term Blackman-Harris window function was used to minimize the spectral leakage, caused by the discretization, and the Inverse Discrete Fourier Transform (IDFT) was applied to obtain the impulsive responses of the channel, $h(t,\tau)$. From them, the power delay profiles $P_h(\tau)$ could be obtained for each one of the 36 measurements of each RX location [3]. In these profiles, the CFAR (Constant False Alarm Rate) technique was applied to clean the noise [14], highlighting and filtering only valid paths through their amplitudes and delays. After pre-processing these data, the average delay parameter $\tau_m$ for MRC characterization was obtained [3]. Thus for each dot of the 6-by-6 quadrangular grid of each measurement RX location, matrices with 36 values of $\tau_m$ were generated.

### B. MRC classification using HMM and Viterbi algorithm

Given its robustness using iterative algorithms, the HMM served as the technical basis for the modeling and analysis of the MRC. In this context, each propagation environment described in this paper (indoor environment, the transition environments outdoor-indoor and indoor-outdoor, as illustrated in Figure 1) had its own radio propagation characteristics and, therefore, were particularly affected by the propagation mechanisms (reflection, scattering, and diffraction). The effects of these phenomena on radio propagation were not directly visible and exposed to observers, so these environments affected by the propagation mechanisms were referred to as hidden states. Likewise, inferences on these hidden states (propagation environments) were carried out through inspections of the values of the MRC temporal dispersion parameter, named average delay ($\tau_m$). Thus, the $\tau_m$ values were referred to as observable states.

Hence, the hidden states were defined as the propagation environments and, inferences about these environments and the respective effects of the propagation mechanisms were revealed through the examination of secondary incidents, designated as the average delay values ($\tau_m$) and described as observable states in the context of the HMM.

The matrices with 36 values of $\tau_m$ from two different RX locations were grouped, with the purpose of comparing and classifying these two propagation environments, resulting in a total of 72 values. For each propagation environment, the 36 values were randomly divided in half between training base and test base. The training bases were grouped (36 random values, 18 from each propagation environment) and used for initialization and training the HMM, while the test bases were grouped (other 36 random values, 18 from each propagation environment) and used to test the HMM trained model, checking if the Viterbi algorithm would be able to correctly classify the $\tau_m$ values from each propagation environment. Then confusion matrices were used to compare the true class (real values belonging to the test base) and the predicted class (optimal sequence of hidden states computed by Viterbi algorithm). The above procedure can be summarized as a pseudocode, as indicated in Table III.

TABLE III. *PROCEDURE SUMMARIZED AS A PSEUDOCODE.*

| Pseudocode | Pseudocode output |
|---|---|
| 1. Select two different RX locations to be compared. | Comparison between two propagation environments (between two hidden states). |
| 2. Calculate $\tau_m$ for each dot at the 6-by-6 quadrangular grid. | Observable states (72 values of $\tau_m$ for both propagation environments). |
| 3. Randomly divide in half the values of $\tau_m$ from each propagation environments. | Creation of:<br>- Trainig base.<br>- Test base. |
| 4. Run HMM initialization and training using training base. | Trained HMM. |
| 5. Run Viterbi algorithm using trained HMM and test base. | Optimal sequence of hidden states (optimal path). |
| 6. Compute the confusion matrix to compare true classes and predicted classes. | Confusion matrix for evaluating the accuracy of the classification. |

Furthermore, in the training stage, the stopping criterion could be a limited number of iterations, a value of improvement in likelihood compared to the previous parameters, or even a combination of the two previous criteria. That way, the number of 100 iterations was used to train and maximize the model parameters, and it also served as stopping criterion.

## V. MODEL EVALUATIONS AND RESULTS

As previously described, at each selected RX location, the reception equipment was set up to acquire the impulse response at each dot of 6-by-6 quadrangular grid, and hence also the respective power delay profiles and the temporal dispersion parameter (average delay $\tau_m$) of each one of the 36 dots of each RX location. After that, the HMM and Viterbi algorithm were used to compare and classify different RX locations. The model evaluations and results were summarized as below.

### A. Evaluation 1 – Comparison between propagation environments: indoor and indoor-outdoor

Evaluation 1 looked closely the transmissions from $TX_1$ to $RX_1$ (indoor-outdoor) and from $TX_1$ to $RX_2$ (indoor), as shown in Figure 1. Therefore, in view of each transmission, 36

temporal dispersion parameters of $\tau_m$ were measured for each RX location (total of 72 values), and after randomly divided in half between training base (36 values) and test base (36 values). The former was used for initialization and training the HMM, while the latter was used for testing the trained model and checking through confusion matrix, if the Viterbi algorithm was able to classify $TX_1$ to $RX_1$ as indoor-outdoor, and $TX_1$ to $RX_2$ as indoor.

TABLE IV. *CONFUSION MATRIX FOR THE EVALUATION 1.*

| True Class \ Predicted Class | Indoor | Indoor-Outdoor |
|---|---|---|
| Indoor | 17 (94.44 %) | 1 (5.56 %) |
| Indoor-Outdoor | 0 (0 %) | 18 (100 %) |

Based on that, it can be seen in Table IV that the HMM and Viterbi algorithm succeeded in hitting 35 (97.22 %) of 36 tested values.

### B. *Evaluation 2 – Comparison between propagation environments: indoor-outdoor and outdoor-indoor*

Evaluation 2 examined the transmissions from $TX_1$ to $RX_1$ (indoor-outdoor) and from $TX_2$ to $RX_3$ (outdoor-indoor), as shown in Figure 1. As applied to evaluation 1, in consideration of each transmission, 36 temporal dispersion parameters of $\tau_m$ were measured for each RX location (total of 72 values), and after randomly divided in half between training base (36 values) and test base (36 values). The former was used for initialization and training the HMM, while the latter was used for testing the trained model and checking through confusion matrix, if the Viterbi algorithm was able to classify $TX_1$ to $RX_1$ as indoor-outdoor, and $TX_2$ to $RX_3$ as outdoor-indoor.

TABLE V. *CONFUSION MATRIX FOR THE EVALUATION 2.*

| True Class \ Predicted Class | Indoor-Outdoor | Outdoor-Indoor |
|---|---|---|
| Indoor-Outdoor | 18 (100 %) | 0 (0 %) |
| Outdoor-Indoor | 2 (11.11 %) | 16 (88.89 %) |

As regards that, it can be seen in Table V that the HMM and Viterbi algorithm succeeded in hitting 34 (94.44 %) of 36 tested values.

## VI. CONCLUSION

The wireless communication systems, generation after generation, have evolved to support the technological breakthroughs and new mobile trends. The MRC characterization is becoming increasingly important in this scenario, due to fact that MRC places huge limitations on the performance of wireless communication systems. In this context, the HMM technique and Viterbi algorithm proved to be initially effective characterizing the MRC and classifying different radio propagation environments.

As further research, it is possible to go ahead, and extended this work with new results as using a combination of temporal dispersion parameters as average delay ($\tau_m$) and delay spread ($\sigma_T$) that can create a better understanding of the phenomenon and consequently a better score, reaching higher values in the classification of radio propagation environments. Other possible actions could be the comparison with other classification models, or the comparison between the HMM modeling using observable states directly connected to hidden states or associated with transitions between hidden states. Or even, study the use of this technique as a classification system that identifies the environment and adjust the parameters of user equipment, such as cell phones, to achieve better transmission and reception results.

## ACKNOWLEDGEMENTS

The authors thank the National Council for Scientific and Technological Development (CNPq, Brazil).

## REFERENCES

[1] GSMA Intelligence Report: *The Mobile Economy*, 2025.

[2] T. S. Rappaport, *Wireless communications principles and practice.* 2nd ed., Prentice Hall Professional Technical Reference, 2002.

[3] J. D. Parsons, *The Mobile Radio Propagation Channel*, 2nd ed., John Wiley & Sons Inc., 2000.

[4] L. G. Ribeiro, L. J. Matos, E. Cataldo, "Aplicação de modelos ocultos de Markov na modelagem do canal rádio móvel". MOMAG2020, 2020, Niterói. 19th Brazilian Symposium of Microwave and Optoelectronics (SBMO) and 14th Brazilian Congress of Electromagnetism (CBMAG), Niterói, Brazil, vol. 1, pp. 296-300, 2021.

[5] R. S. Azevedo, L. J. Matos, E. Cataldo, "Aplicação dos modelos ocultos de Markov na caracterização banda larga do canal rádio indoor", 2022 XL Brazilian Telecommunications Symposium (SBrT'22), Santa Rita do Sapucaí, Brazil, 2022. DOI: 10.14209/sbrt.2022.1570804884.

[6] R. S. Azevedo, L. J. Matos, E. Cataldo, "Use of Hidden Markov Model Technique to Characterize and Classify the Wideband Mobile Radio Channel in Different Environments", Journal of Microwaves, Optoelectronics and Electromagnetic Applications (JMOe), Vol. 23, No. 1, 2024. DOI: https://dx.doi.org/10.1590/2179-10742024v23i1276299.

[7] L. R. Rabiner, B. H. Juang, "An Introduction to Hidden Markov Models". IEEE ASSP Magazine, 3, 4-16., 1986.

[8] J. P. Coelho, T. M. Pinho, J. Boaventura-Cunha, "Hidden Markov Models: theory and implementation using Matlab®", CRC Press Inc., 2019.

[9] F. M. Silveira, C. Schueler, E. Cataldo, "Utilização da técnica MFCC em conjunto com os parâmetros extraídos do sinal glotal para melhorar o desempenho de um sistema de verificação de locutor", XXXV Brazilian Telecommunications Symposium (SBrT'17), São Pedro, Brazil, 2017.

[10] F. J. S. Campos, *Modelos ocultos de Markov: del reconocimiento de voz a la música*, Granada Univ., 2007.

[11] L. R. Rabiner, "A Tutorial on HMM and Select App in Speech Recognition", Proc. IEEE, Vol. 77, n. 2, Feb. 1989.

[12] C. F. Souza, J. C. R. Dal Bello, "Aplicação da técnica de sondagem em frequência na caracterização de canais de UWB exteriores", XXVI Brazilian Telecommunications Symposium (SBrT'08), Rio de Janeiro, Brazil, 2008.

[13] A. B. Poritz, "Hidden Markov Model: A Guided Tour", Porc. of the IEEE Int. Conf. on in Acoustics, Speech, and Signal Processing, pp. 7-13, 1988.

[14] L. J. Matos, B. S. Marinho, "A comparison of the delay spread obtained with different power delay profiles de-noising techniques", Engevista, vol. 13, n. 2, pp. 129-133, 2011.